



# A multi-stable lattice structure and its snap-through behavior among multiple states

Fuhong Dai <sup>\*</sup>, Hao Li, Shanyi Du

Center for Composite Materials and Structures, Harbin Institute of Technology, Harbin 150001, China

## ARTICLE INFO

Article history:  
Available online 5 November 2012

Keywords:  
Multi-stable  
Lattice structure  
Snap through  
Bistable laminates  
Critical load

## ABSTRACT

This paper develops a multi-stable lattice structure consisting of tri-stable lattice cell which is made by bistable laminates. The multi-stable lattice structure with  $N$  tri-stable lattice cells, which can exhibit  $2^N$  stable states, is successfully designed and fabricated. The critical loads snapping lattice structure are investigated by the experimental and finite element techniques. The method to simulate the behaviors of contact and constraint between the neighboring bistable laminates are presented. The snap through process of multi-stable lattice structures among multiple states are numerically simulated and experimentally validated. The multiple stabilities highlight the potential to achieve a smooth shape variation in the large area multi-stable structures.

Crown Copyright © 2012 Published by Elsevier Ltd. All rights reserved.

## 1. Introduction

Multi-stable structures are growingly becoming attractive in developing morphing and deployable structures [1–3], since they are able to sustain significant changes in shape without the need for a continuous power supply. Bistable materials such as thermal-stress-based bistable laminates [4–10] and prestress-based bistable shell [11–14] are the most fundamental components in multi-stable structures.

Since 1981, many works on bistable laminates have been published. The cured curvature of bistable laminates can be predicted with good precision by using analytical approaches [15–17]. In addition, finite element analyses are a robust way to predict cured shape and to simulate the snap through process [18–20].

To induce the snap-through process from one stable state to another, the actuator materials such as shape memory alloy and piezoelectric composites [21–23] have been employed. An adaptive prototype of a multi-stable composite with integrated smart alloys had been designed and manufactured by Hufenbach et al. [24]. Dano studied theoretically and experimentally the concept of using shape memory alloy wires to effect the snap-through of unsymmetric composite laminates [25]. The concept of morphing and deployable structures based on a piezoelectric Macro-Fiber Composite (MFC) actuator have been presented by Schultz et al. [26] and Tawfik Samer et al. [27]. Giddings combined a finite element model of an MFC with a bistable asymmetric laminate model. Both the pre-

dicted shape and the snap-through voltage of a piezo-actuated [0/90] laminate compared well with the experimental results [28].

The interests have been recently extended to study the dynamic behavior of bistable laminates. Vogl and Hyer centered on the lowest natural frequency and the associated mode shape for laminates clamped at their midpoints, with special attention as to how these vibration characteristics depend on the laminate side-length-to-thickness ratio [29]. Arrieta analytically and experimentally investigated the dynamics of cross-well oscillations and the key dynamic features of snap-through [30].

There might be the requirement of the capacity transforming among multiple states in some applications such as in variable sweep wing and morphing airfoil to achieve aerodynamic performance gains [31]. In 2007, Mattioni et al. demonstrated that the laminate with piecewise variation of the lay-up in the plan-form can be multi-stable and a variable camber trailing edge resulting in four equilibrium configurations was presented [31]. They also addressed that the piecewise variation of the lay-up may lead to unpredictable interactions between each stable state therefore care must be exercised when considering multi-stable structures. Most recently, a multi-stable composite twisting structure capable of large deformations, simply consisting of two prestressed flanges joined to introduce two stable configurations has been explored by Lachenal et al. [32]. They presented a prototype with multiple configurations: (a) the straight, (b) the twisted and (c) the coiled configuration. But a sufficient friction is needed to hold the straight unstable configuration, a thin wire holding the structure in its coiled unstable configuration.

To overcome the difficulty to precisely control the complicated piecewise layups and to avoid the external force to hold the stable

<sup>\*</sup> Corresponding author.

E-mail address: [daihf@hit.edu.cn](mailto:daihf@hit.edu.cn) (F. Dai).

configuration, a possible solution is to construct the multi-stable structures by assembling the simple bistable laminates.

This paper developed a multi-stable lattice structure that can be snapped among different states. The multi-stable lattice structure consists of the tri-stable lattice cells which can offer three stable configurations. The critical loads snapping lattice are investigated by the experimental and finite element techniques. Finally, the snap through process of multi-stable lattice structure among multiple states are numerically simulated and experimentally validated.

## 2. Design and fabrication of multi-stable lattice structures

The first step to construct a multi-stable lattice structure is to find a bistable component that is fit to be assembled with each other and the connection technique which has none or little influence on the bistability of the neighboring components. Through the experimental study, we found that the longer rectangular bistable laminate with the length several times width is an appropriate candidate of such components. The two rectangular bistable laminates in extended states are bonded by a bolt near the short edge, the four rectangular bistable laminates assembling a tri-stable lattice cell. The assembling lattice cell exhibits an initial plane geometric configuration, see Fig. 1a. A plane stable configuration is difficult to achieve through manipulating the lay-ups of laminates. The hole where the bolt is mounted is small enough not to influence the bistability of the connecting bistable laminates. Each rectangular laminate is designed to obtain the equal magnitude of curvatures at two stable states (extended and bent configurations), which results in the close and smooth contact when the lattice cell is bent to be the concave and convex configurations, see Fig. 1b and c.

The multi-stable lattice structure can be obtained by adding the more rectangular bistable laminates to the lattice cell. For example, a multi-stable lattice structure consisting of two lattice cells gives four stable configurations, see Figs. 2 and 3. It is noted that the direction of additionally added rectangular laminates should be carefully chosen. Different connection modes of neighboring rectangular laminates may lead to different multiple stable states. The same concave configuration between two neighboring rectangular laminates in longitudinal direction leads to four stable geometric configurations, as seen in Fig. 2, while the different geometric configuration (one concave and another convex) results in four stable configurations as seen in Fig. 3. Considering the interaction of one lattice cell with neighboring lattice cell, the introduction of one tri-stable cell gives the structure two equilibrium configurations and it is (in principle) possible to obtain  $2^N$  configurations by using  $N$  tri-stable lattice cells.

Several multi-stable lattice structures are fabricated. The material properties are listed as in Table 1. The size of each rectangular bistable laminate is 140 mm × 35 mm × 0.25 mm with a stacking sequence of [0/90]<sub>7</sub>. In the experiment, we first manufactured a

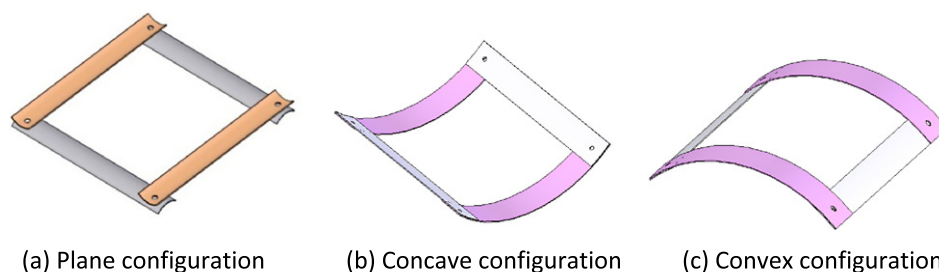


Fig. 1. Three stable geometric configurations of tri-stable lattice cell.

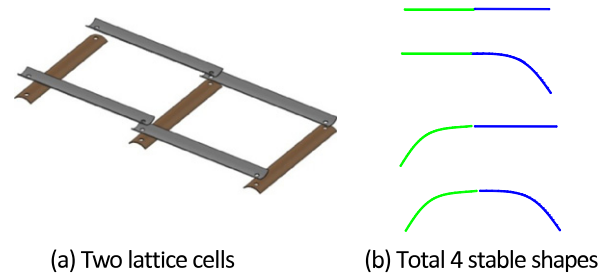


Fig. 2. The four stable lattice structure with the same configurations between neighboring rectangular laminates in longitudinal direction.

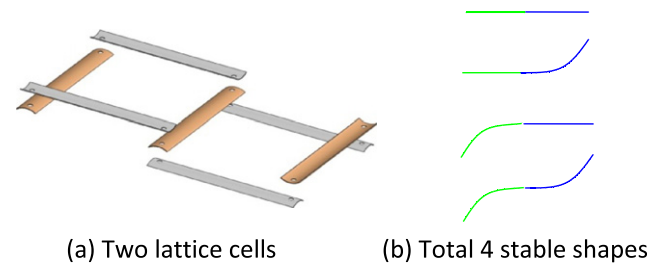


Fig. 3. The four stable lattice structure with different configurations between neighboring rectangular laminates in longitudinal direction.

Table 1

Material properties of CFRP.

|      |  |
|------|--|
| CFRP | $E_{11} = 137.47$ GPa, $E_{22} = 10.07$ GPa, $G_{12} = 7.17$ GPa, $\nu_{12} = 0.23$ ,<br>$\alpha_{11} = 0.37 \times 10^{-6}$ °C, $\alpha_{22} = 24.91 \times 10^{-6}$ °C, Thickness = 0.125 mm |
|------|--|

square laminate of 150 mm × 150 mm × 0.25 mm by an autoclave technique. Then, the square laminate was cut into four same size rectangular laminates. It is reported that the laminate may lose internal thermal stress and the snap-through load decreases obviously due to the moisture effect [33]. The bistable laminates used in experiments have been exposed in the air and the effect of moisture should not be neglected. To quantify the effect of moisture, we retested the bistable laminate by heating it and found that it regained a flat shape when the temperature raised to 160 °C, which is 20 °C lower than the curing temperature of laminate, 180 °C. It is convenient to take consideration of moisture effect in FEA by decreasing the initial curing temperature. Therefore, the finite element models of the bistable laminates are numerically generated during the cool-down process using 160 °C as the initial temperature and the room temperature 20 °C as the final temperature.

The four components of the lattice structure are connected by the bolts. Although the holes must be drilled into the bistable laminates to fix the bolts, the holes only affect the stress distribution locally and have little influence on the bi-stability of the laminate.

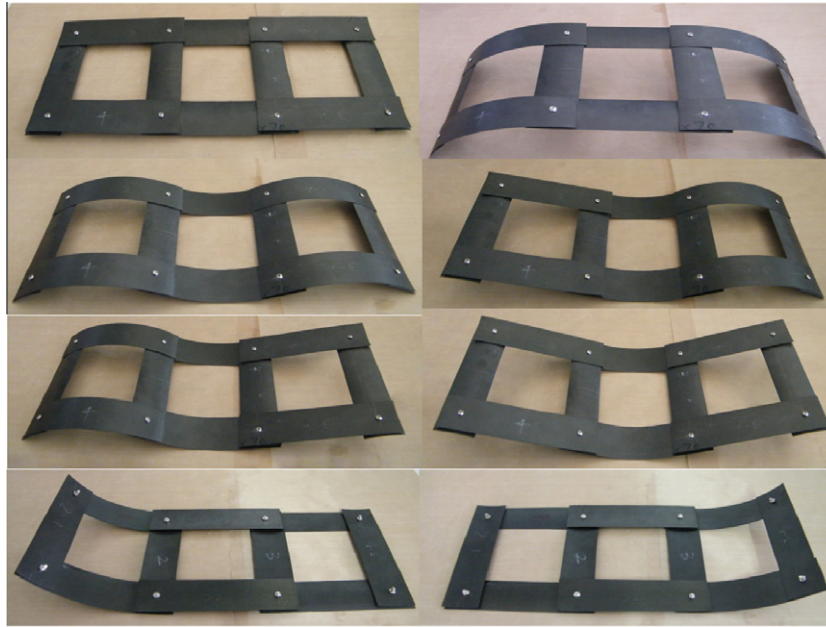


Fig. 4. The eight stable lattice structure with three lattice cells.

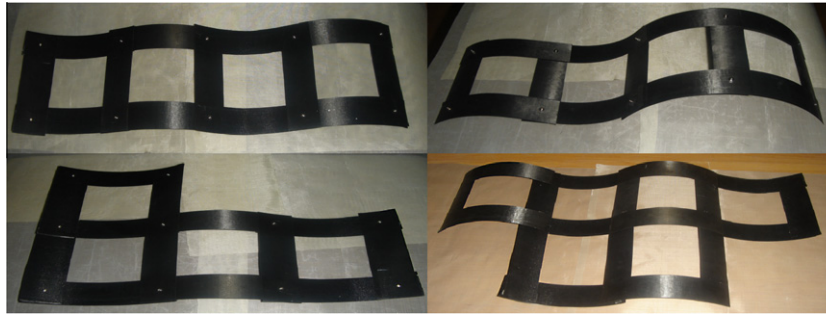


Fig. 5. Fabricated multi-stable lattice structures with four and six lattice cells.

A multi-stable lattice structure consisting of the three lattice cells and its total eight stable geometric configurations are shown in Fig. 4. Fig. 5 presents the examples of multi-stable lattice structures with four and six lattice cells.

### 3. Measurement of critical loads

The experiments are conducted to test the critical loads to snap the tri-stable lattice cell in this section. A lattice cell used consists of four rectangular laminates, which have the size of  $140 \text{ mm} \times 35 \text{ mm} \times 0.25 \text{ mm}$  and stacking sequence of  $[0/90]_T$ . The multi-stable lattice structures are snapped among different states by applying external force on the lattice cell. Considering it is easier way to snap the lattice cell by applying the moment than by applying the concentrated force, the snapping moment is tested. The lattice cell is clamped at one end and the loads are applied at another end, see Fig. 6. In experiments, the force at the end of the cantilever structure is recorded by gradually adding water in a small container until the snap-through is induced. The total four samples are tested and the force is measured to be  $0.163 \pm 0.007 \text{ N}$ . Then the critical moment to snap the lattice cell is obtained by multiplying the force by the distance from the supports of  $135 \text{ mm}$ , which is  $0.022 \text{ Nm}$ . The same testing procedure is also used to measure the critical moment of single rectangular laminates, which is  $0.013 \text{ Nm}$ . As

expected, the lattice has almost twice critical load as the single rectangular laminate. The similar phenomenon was reported in the literature [34] where more critical load's tests can be found. There are three rectangular laminates bonding together in the multi-stable lattice structure. At this case, the bonding should carefully be designed not to influence the bi-stability of laminates. Especially for the connecting design as shown in Fig. 3, the longitudinal rectangular laminates will locally lose the stability if the three rectangular laminates are fully bonded together by bolts. The bolts should be fastened tightly enough to constrain their mutual movements and not to have significant influence on their snap-through. Therefore, we do further tests to examine effects of the tightness of bolts on critical moments and the little difference of critical moments is observed in experiment. This may be due to the fact that the bonding area is very small and the bonding effect acts only near the bolts.

### 4. Numerical simulation methods

For complex structures it is necessary to employ numerical methods such as finite elements to determine the multi-stability. A numerical procedure to identify the equilibrium shapes and the structural response of bistable structures has been established with the commercial software ABAQUS. This simulation technique is divided into two steps: the first that reproduces the cool-down

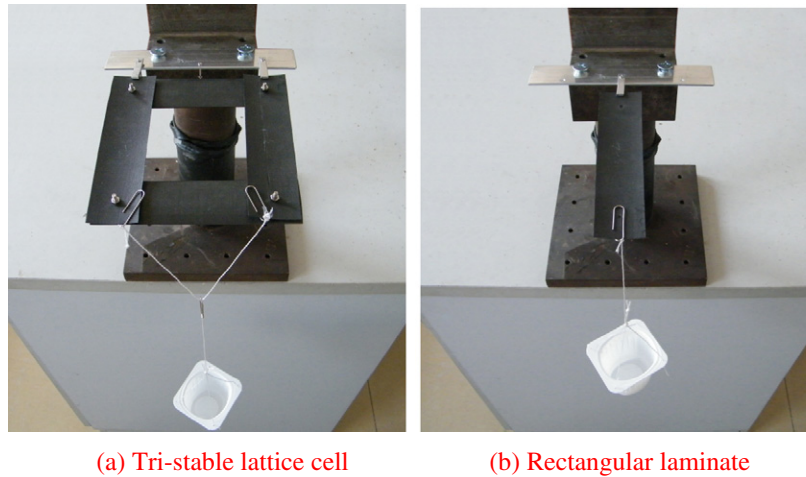


Fig. 6. Measurement of critical loads for tri-stable lattice cell and bistable rectangular laminate.

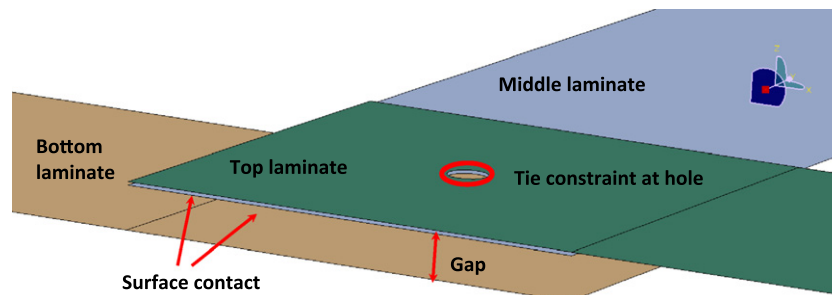


Fig. 7. Local bonding region of three rectangular laminates.

Table 2

Convergence of critical moments with the coefficient of friction.

| The coefficient of friction | Critical moments (Nm) |
|-----------------------------|-----------------------|
| 0                           | 0.0207                |
| 0.125                       | 0.0207                |
| 0.250                       | 0.0207                |
| 0.325                       | 0.0207                |
| 0.500                       | 0.0208                |

after the curing. The second step, the snap-through analysis, describes the elastic response of the structure when loaded.

Here, we use finite element method to solve the nonlinear problems of snap-through in multi-stable structures and predict each equilibrium configuration. The calculation is performed with ABAQUS in two steps as well. In first step, the cool-down analysis is carried out to generate an initial lattice structure that consists of multiple tri-stable lattice cells and is allowed to be snapped among multiple states. In second step, the snap-through process is simulated when loaded. During the application of the load, the structure will first deform elastically. Then, once the load reaches a critical value, it will collapse and eventually rest on the other stable configuration when the load is removed. The problem represents an unstable collapse and arc-length methods are considered to be the preferred tool.

The analysis is performed using 4-node general purpose reduced integration shell elements (S4R) and geometrically nonlinear algorithms (NLGEOM). To avoid instabilities in the model due to snap-through the STABILIZE command is used in ABAQUS/Standard with a damping factor of  $1 \times 10^{-6}$ . The detail discussion about the influence of the damping factor can be found in the

literature [9]. The lattice cell is modeled using a composite shell section to enable the use of a single layer of S4R elements. Total 5756 elements are used to model the curing shape and the snap-through behavior. Convergence studies show that both a mesh with 5756 elements and a finer mesh with 22,404 elements give the same curvature of  $8.8 \text{ m}^{-1}$  and same critical moment of 0.0207 Nm.

The specific issues for multi-stable lattice structures are the interactions between two neighboring bistable laminates due to their bonding and contact. The finite element model should be effective to simulate both the cool down and snap through process. The local bonding region of three rectangular laminates, which is flat and established before cool down, is shown as in Fig. 7. ABAQUS/Standard provides several options for modeling contact and interaction problems. At first, the tie constraints are imposed on the nodes at holes to simulate the bonding constraints. Then, the surface-to-surface contacts are defined to explain the interaction between two neighboring laminates. The initial model of each rectangular laminate will deform to a cylindrical shell after cool down, the top laminate bending up, the middle laminate bending down and the bottom laminate bending up. The full contact between the top laminate and the middle laminate is able to allow thus deformation whereas a gap between the middle laminate and the bottom laminate has to be adopted to allow them to deform to cylindrical shapes. The contact properties between two surfaces can be chosen based on the geometric and loading conditions. Mechanical contact property includes the constitutive model, the damping model and the friction model. Since the deformation of the multi-stable lattice structure in this study is assumed to be a quasi-static problem, only friction property should be considered. The influence of friction coefficient on convergence of critical mo-



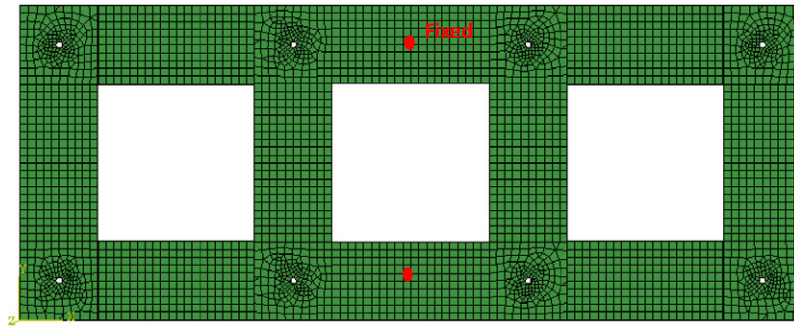


Fig. 8. Finite element model and assembling pattern of a multi-stable lattice structure with three cells.

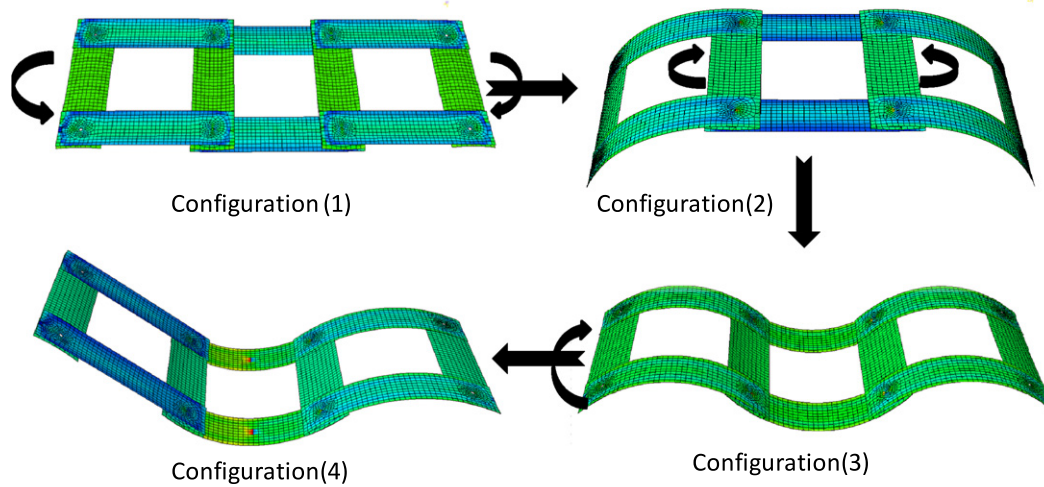


Fig. 9. Four stable geometric configurations simulated by FEM of a multi-stable lattice structure with three cells.

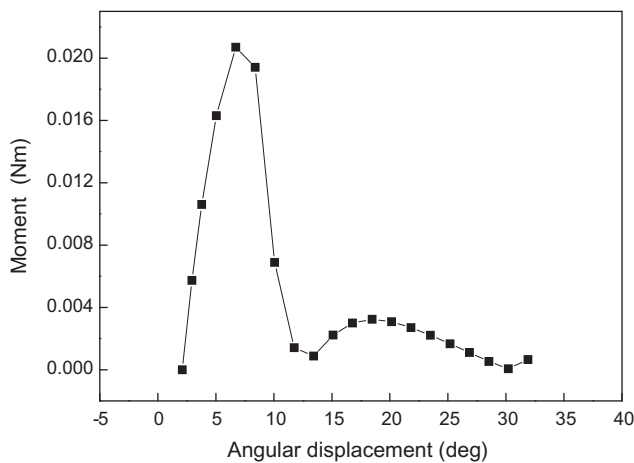


Fig. 10. Moments vs. angular displacements at the end of lattices by FEM.

Table 3

Simulated and measured critical moments to snap the lattice cell.

| Specimens                      | 1      | 2      | 3      | 4      | Average |
|--------------------------------|--------|--------|--------|--------|---------|
| Measured critical moment (Nm)  | 0.0212 | 0.0225 | 0.0225 | 0.0215 | 0.0219  |
| Simulated critical moment (Nm) | 0.0207 |        |        |        |         |
| Error (%)                      | 2.3    | 8.0    | 8.0    | 3.7    | 5.4     |

in finite element analysis are illustrated as in Fig. 8. The structure consists of ten rectangular laminates and is made by putting ten pieces of rectangular laminates together. The bonding is simulated by “tie” constraint technique and the totally twelve surface-to-surface contacts are established between two neighboring laminates. As mentioned above, since the lap regions are bonded by bolts and the relative movements between different laminates are restricted, the contact properties with no friction effect are used. The diameters of holes are all 3 mm according with the experimental sizes. The gap between middle laminates and bottom laminates as mentioned above is chosen to be 3 mm which does not only allow laminates to deform to cylindrical shape but also enable the deformed laminates remain contact with each other. The materials used are listed in Table 1. The two points at the center of middle rectangular laminates are fixed, see Fig. 8.

Fig. 9 presents four stable geometric configurations corresponding to the first four experimental shapes in Fig. 4. Configuration (1) is flat and obtained after cool down. The rectangular laminates bend in the direction of short edge and remain the bistability. Then

ments to snap the lattice cell is listed in Table 2. It shows the change of friction factor has little influence on the convergence. So, the contact property with no friction effect is adopted.

## 5. Results

The multi-stable lattice structure with three lattice cells, as seen in Fig. 4, is investigated to illustrate the snap through among multiple states. The finite element model and assembling pattern used

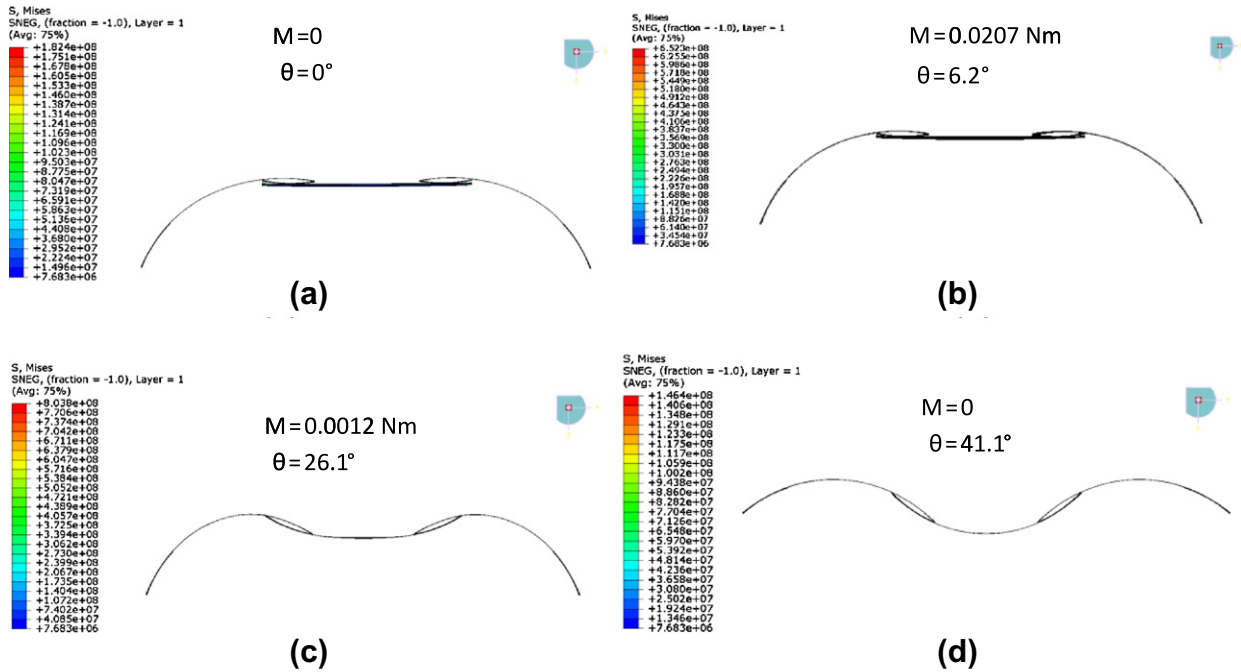


Fig. 11. Simulated snap-through process from configuration (2) to configuration (3),  $M$  represents the moment and  $\theta$  indicates the angular displacement.

a new analysis step is restarted using the results of cool down analysis as the initial condition. By applying the moments at two ends of the multi-stable lattice, it will be snapped into configuration (2). Since the rectangular laminates have equal curvatures in two directions, the snapped rectangular laminates in longitudinal direction fully contact with the neighboring transverse rectangular laminates in the left and right lattices. In the following up step, a new analysis using configuration (2) as initial condition is carried out. The loads applied in last step are removed and new loads are applied at the two ends of middle lattice. The multi-stable lat-

tice structure is transformed from configuration (2) to configuration (3). The rectangular laminates are all bending in longitudinal direction in the configuration (3) and a smooth wavy lattice can be observed. In final step, modifying the initial condition and removing the last step's loads, configuration (3) is shifted to be configuration (4) with the application of the moment at left end, which has an opposite sign to that applied in configuration (1). The left lattice recovers to its initial flat state after cool down. The other two lattices remain the concave and convex geometric configurations respectively.

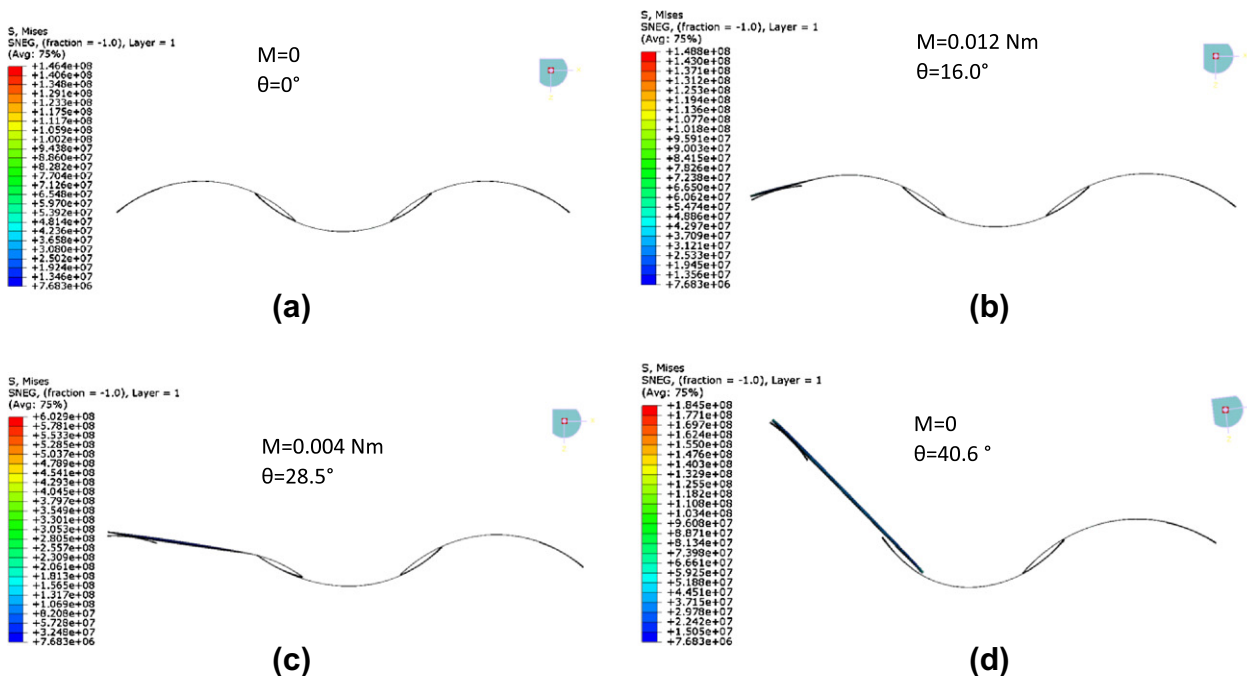


Fig. 12. Simulated snap-through process from configuration (3) to configuration (4),  $M$  represents the moment and  $\theta$  indicates the angular displacement.

The curve of moments vs. angle displacements for a lattice structure from the plane configuration to the concave configuration by FEM is plotted in Fig. 10. It can be observed that the snap-through occurs when the moment reaches to a critical magnitude of 0.0207 Nm where the angular displacement is 6.2°. The finite element analysis also captures the unloading process which is difficult to be identified by experiments. The displacements still increase during unloading process and a maximum angle displacement is up to 32.1°, at which the lattice rests on new stable state. We have measured the critical moments for four lattice samples and the average measured critical moment is 0.0219 Nm. The deviation of predicted critical moment from the experimental one is 5.4%. The comparison between the predicted and experimental critical moments is presented in Table 3. It is noted that each lattice should have the consistent critical moment since it is periodic.

The snap-through processes for configurations (2–4) are illustrated in Figs. 11 and 12 and the Von Mises stresses are included in the figures. The moment and angular displacement with respect to each shape are presented in Figs. 11 and 12 as well, which shows the deformation gradually increases with the load changes. Fig. 11 demonstrates the shape change of middle lattice from the plane configuration to the concave configuration. At this case, the two lattices at its left and right sides exhibit as a rigid body movement and have little influence on its snap through behavior except their gravities. The maximum stress remains at the holes of the middle lattice. Fig. 11b illustrates the critical state at which the moment reaches to the critical value of 0.0207 Nm. Fig. 11c and d shows the shape change during unloading. It can be seen that the deformation of lattice cell still increases until it rests on the new stable state although the load decreases. Fig. 12 demonstrates the shape change of left lattice from the convex configuration to the plane configuration. Similarly, the snap through of left lattice is almost independent on the other two lattices. The location where the maximum stress occurs shifts from the holes to the central point of middle rectangular laminates at which the model is fixed. Fig. 12b illustrates the critical state at which the moment reaches to the critical value of 0.012 Nm, which is almost half of the critical moment from the plane configuration to the concave configuration. The similar phenomenon can be found in the Ref. [34]. Fig. 12c and d shows the shape change during unloading. When the moment decreases to zero and the maximum angular displacement increases to 40.6°, the cell rests on the new stable state.

The snap through processes of other configurations can be simulated by using the present method. It is clearly observed that the rectangular laminates in longitudinal direction are bendable and the rectangular laminates in transverse direction only act as the connectors. If adding more lattices in transverse direction, they also can be snapped into another state depending on the assembling pattern and the bonding design.

## 6. Conclusions

A multi-stable lattice structure has been developed in this study. At first, the longer rectangular bistable laminate with the length several times width is used to construct a tri-stable lattice. Then the multi-stable lattice structure is assembled by using tri-stable lattice cell. The bolts are employed to bond the rectangular laminates together and it shows that the connection has little influence on the bistability of the neighboring components. Two different connection modes of neighboring rectangular laminates, which may lead to different geometric configurations, are presented. Several multi-stable lattice structures are designed and fabricated. Considering the interaction of one lattice cell with neighboring lattice cell, the introduction of one tri-stable cell gives the structure two equilibrium configurations and it is (in principle)

possible to obtain  $2^N$  configurations by using  $N$  tri-stable lattice cells. The concept is validated with an example of a multi-stable lattice structure with three lattice cells, which exhibits eight stable geometric configurations.

The “tie” constraint and surface-to-surface contact are used to simulate the interactions between two neighboring bistable laminates due to their bonding and contact. The friction effect has little influence on the snapping loads of lattice cell. The critical loads are experimentally measured and numerically predicted using finite element method. The predicted critical moment of the lattice cell is 0.0207 Nm, which results in an error 5.4% compared with the experimental result. The finite element analysis captures the unloading process and the deformation during snap-through, which is difficult to be observed in experiments. Taking a multi-stable lattice consisting three lattice cells as an example, the continuous shape change among four stable geometric configurations are successfully simulated. It shows that the cells with no loading exhibit as a rigid body movement and have little influence on the snap through behavior of the cell loaded except the gravity. A full and smooth contact between the longitudinal and transverse laminates is demonstrated and the smooth multi-stable wavy lattice can be obtained, when the lattice deforms to the concave or convex configuration. The results show that the multiple stabilities highlight the potential to achieve a smooth shape variation in the large area multi-stable structures.

## Acknowledgements

This work was supported by National Natural Science Foundation of China (Grant Nos. 10502016 and 10872058) and Laboratory of Science and Technology on Advanced Composites in Special Environments.

## References

- [1] Bowen CR, Butler R, Jervis R, et al. Morphing and shape control using unsymmetrical composites. *J Intell Mater Syst Struct* 2007;18:89–98.
- [2] Lei YM, Yao XF. Experimental study of bistable behaviors of deployable composite structure. *J Reinf Plast Compos* 2010;29:865–73.
- [3] Pirrera A, Avitabile D, Weaver PM. On the thermally induced bistability of composite cylindrical shells for morphing structures. *Int J Solids Struct* 2012;49:685–700.
- [4] Hyer MW. Calculation of the room-temperature shapes of unsymmetric laminates. *J Compos Mater* 1981;15:296–310.
- [5] Hyer MW. The room-temperature shapes of four layer unsymmetric cross-ply laminates. *J Compos Mater* 1982;16:296–310.
- [6] Fuhong Dai, Boming Zhang, Xiaodong He, et al. Numerical and experimental studies on cured shape of thin unsymmetric Carbon/Epoxy composite laminates. *Key Eng Mater* 2007;334–335:137–40.
- [7] Harper BD. The effects of moisture induced swelling upon the shapes of anti-symmetric cross-ply laminates. *J Compos Mater* 1987;21:36–48.
- [8] Gigliotti Marco, Wisnom Michael R, Potter Kevin D. Loss of bifurcation and multiple shapes of thin [0/90] unsymmetric composite plates subject to thermal stress. *Compos Sci Technol* 2004;64:109–28.
- [9] Daynes S, Weaver PM. Analysis of unsymmetric CFRP–metal hybrid laminates for use in adaptive structures. *Composites: Part A* 2010;41:1712–8.
- [10] Betts DN, Salo Aki IT, Bowen CR, Kim HA. Characterisation and modelling of the cured shapes of arbitrary layup bistable composite laminates. *Compos Struct* 2010;92(7):1694–700.
- [11] Norman AD, Guest SD, Seffen KA. Novel multistable corrugated structures. In: 48th AIAA/ASME/ASCE/AHS/ASC Structures, Structural Dynamics, and Materials Conference 15th, Honolulu, Hawaii, AIAA 2007–2228, 23–26 April 2007.
- [12] Kebabdz E, Guest SD, Pellegrino S. Bistable prestressed shell structures. *Int J Solids Struct* 2004;41:2801–20.
- [13] Daynes S, Potter KD, Weaver PM. Bistable prestressed buckled laminates. *Compos Sci Technol* 2009;68:3431–7.
- [14] Yokozeki Tomohiro, Takeda Shin-Ichi, Ogasawara Toshio, et al. Mechanical properties of corrugated composites for candidate materials of flexible wing structures. *Composites: Part A* 2006;37:1578–86.
- [15] Jun WJ, Hong CS. Effect of residual shear strain on the cured shape of unsymmetric cross-ply thin laminates. *Compos Sci Technol* 1990;38:55–67.
- [16] Cho Maenghyo, Kim Min-Ho, Choi Heung Soap, et al. A study on the room-temperature curvature shapes of unsymmetric laminates including slippage effects. *J Compos Mater* 1998;32:460–82.

- [17] Pirrera A, Avitabile D, Weaver PM. Bistable plates for morphing structures: a refined analytical approach with high-order polynomials. *Int J Solids Struct* 2010;47:3412–25.
- [18] Samer Tawfik, Xinyuan Tan, Serkan Ozbay, et al. Anticlastic stability modeling for cross-ply composites. *J Compos Mater* 2007;41(11):1325–38.
- [19] Tawfik Samer A, Stefan Dancila D, Armanios Erian. Planform effects upon the bistable response of cross-ply composite shells. *Composites: Part A* 2011;42:825–33.
- [20] Giddings Peter F, Bowen Christopher R, Salo Aki IT, et al. Bistable composite laminates: effects of laminate composition on cured shape and response to thermal load. *Compos Struct* 2010;92:2220–5.
- [21] Betts DN, Kim HA, Bowen CR. Modeling and optimization of bistable composite laminates for piezoelectric actuation. *J Intell Mater Syst Struct* 2011;22(18):2181–91.
- [22] Bowen CR, Giddings PF, Salo Aki IT, et al. Modeling and characterization of piezoelectrically actuated bistable composites. *IEEE Trans Ultrason Ferroelectr Frequency Control* 2011;58(9):1737–50.
- [23] Amancio Fernandes, Corrado Maurini, Stefano Vidoli. Multiparameter actuation for shape control of bistable composite plates. *Int J Solids Struct* 2010;47:1449–58.
- [24] Hufenbach W, Gude M, Kroll L. Design of multistable composites for application in adaptive structures. *Compos Sci Technol* 2002;62: 2201–7.
- [25] Dano ML, Hyer MW. SMA-induced snap-through of unsymmetric fiber-reinforced composite laminates. *Int J Solids Struct* 2003;40:5949–72.
- [26] Schultz MR, Hyer MW, Williams RB, et al. Snap-through of unsymmetric laminates using piezocomposite actuators. *Compos Sci Technol* 2006;66:2442–8.
- [27] Tawfik Samer A, Stefan Dancila D, Armanios Erian. Unsymmetric composite laminates morphing via piezoelectric actuators. *Composites: Part A* 2011;42:748–56.
- [28] Giddings PF, Kim HA, Salo AIT, Bowen CR. Modelling of piezoelectrically actuated bistable composites. *Mater Lett* 2011;65:1261–3.
- [29] Vogl GA, Hyer MW. Natural vibration of unsymmetric cross-ply laminates. *J Sound Vib* 2011;330:4764–79.
- [30] Arrieta AF, Neild SA, Wagg DJ. On the cross-well dynamics of a bi-stable composite plate. *J Sound Vib* 2011;330:3424–41.
- [31] Mattioni F, Weaver PM, Friswell MI. Modelling and applications of thermally induced multistable composites with piecewise variation of lay-up in the planform. In: 48th AIAA/ASME/ASCE/AHS/ASC Structures, Structural Dynamics, and Materials Conference 15th, Honolulu, Hawaii, AIAA 2007–2262, 23–26 April 2007.
- [32] Lachenal X, Weaver PM, Daynes S. Morphing applications multi-stable composite twisting structure for morphing applications. *Proc. R. Soc. A*, 4 January 2012 [doi: 10.1098/rspa.2011.0631Z].
- [33] Etches J, Potter K, Weaver P, Bond I. Environmental effects on thermally induced multistability in unsymmetric composite laminates. *Compos A* 2009;40:1240–7.
- [34] Dai F, Li H, Du S. Design and analysis of a tri-stable structure based on bi-stable laminates. *Composites: Part A* 2012;43:1497–504.